Spring 2022

Characterization of Nanoparticles Using Inductively-Coupled Plasma Mass Spectrometry

Jabez D. Campbell
Missouri State University, Jabez118@live.missouristate.edu

CHARACTERIZATION OF NANOPARTICLES USING INDUCTIVELY – COUPLED PLASMA MASS SPECTROMETRY

A Master's Thesis

Presented to

The Graduate College of

Missouri State University

In Partial Fulfillment

Of the Requirements for the Degree

Master of Science, Chemistry

By

Jabez Campbell

May 2022

CHARACTERIZATION OF NANOPARTICLES USING INDUCTIVELY – COUPLED PLASMA MASS SPECTROMETRY

Chemistry

Missouri State University, May 2022

Master of Science

Jabez Duane Campbell

ABSTRACT

Nanomaterials are a relatively new class of materials that have many applications which span a wide host of fields from medical products to consumer products. The possible compositions and forms of nanomaterials are just as varied as the applications. Therefore, a versatile characterization method is needed for researchers and regulators alike to ensure nanomaterials are properly used. Single Particle Inductively Coupled Plasma Mass Spectrometry (SP-ICP-MS) is a functional method that could fill the characterization need in the nanomaterial research field. Using data from both SP-ICP-MS tests and data from literature established characterization methods, the viability of making SP-ICP-MS the standard method was assessed. Initially, the data from the SP-ICP-MS seemed to vary significantly from the expected results until the data was checked against the conventional methods. After the comparison, the variance in the data appeared to come from the nanoparticles used in the study instead of the testing method. Then the data from SP-ICP-MS was analyzed using Excel, in accordance with the manufacturer's application manual, in an attempt to recreate the observed results with limited success. In the end, the viability of SP-ICP-MS as a standard characterization method was not confirmed in practice because there were optimization issues and software problems that have not yet been resolved.

KEYWORDS: nanomaterial, nanoparticle, characterization, SP-ICP-MS, standard

CHARACTERIZATION OF NANOPARTICLES USING INDUCTIVELY – COUPLED PLASMA MASS SPECTROMETRY

By

Jabez Duane Campbell

A Master's Thesis
Submitted to the Graduate College
Of Missouri State University
In Partial Fulfillment of the Requirements
For the Degree of Master of Science, Chemistry

May 2022

Approved:

Richard Biagioni, Ph.D., Thesis Committee Chair

Erich D. Steinle, Ph.D., Committee Member

Kartik C. Ghosh, Ph.D., Committee Member

Gautam Bhattacharyya, Ph.D., Committee Member

Julie Masterson, Ph.D., Dean of the Graduate College

ACKNOWLEDGEMENTS

I dedicate this thesis to my wife, Sarah Campbell.

For all of the patience, grace, and support she has given me while I have completed this accomplishment.

TABLE OF CONTENTS

LIST OF TABLES

LIST OF FIGURES AND EQUATIONS

INTRODUCTION

Nanomaterials

Nanomaterials are a class of materials that is currently under heavy investigation and also some scrutiny[1]. Nanomaterials are classified as any material that has at least one dimension that is 100 nanometers or less[1]. These materials can be composed of any element or any combination of elements and may be shaped in a wide variety of geometric shapes[2]. The common shapes that are observed for natural and engineered nanomaterials are two dimensional planes, geometric shapes, tubules and spherical particles[2]. Of the common shapes, spherical particles are the most frequently observed structure among both natural and engineered nanomaterials[1]. Among the possible compositions the ones most commonly seen in the literature are pure gold, pure silver, and metal oxides[1,3].

The intense investigation of nanomaterials stems from the unique properties that the materials possess[1]. Properties such as cellular toxicity, optical characteristics, and specific reactivity vary greatly when the nanomaterial version of a substance is compared to the bulk form of the same substance[1]. For example, bulk gold is a solid material that has a yellow coloration while nanomaterial gold is a powder or suspension in liquid that has a red to black coloration. Also, nano-silver has increased targeted toxicity to bacterial cells compared to bulk silver when introduced to the human system[1]. These unique properties are indicative of the notion that nanomaterials have wide spanning applications[1].

One problem that has arisen from the widespread applications of nanomaterials is the excessive eagerness of private companies to utilize these materials in products[1]. This eagerness has caused several commercial products that contain nanomaterials to be mass produced and

distributed[1]. The problem comes with the fact that only a few long-term toxicological studies have been conducted on nanomaterials in general[1]. As such, companies are utilizing full airborne containment measures in factories and facilities to ensure worker safety[4]. While these measures depend on the specific company, one common component is the double bagging and dampening of waste materials to make sure that dust from dry waste does not pollute the air even after a significant amount of time[4]. So the question that comes to mind is, how can companies know that a product is safe for the general public when the effects on their workers is not fully known?

The academic community has also been grappling with the issue of understanding the long-term effects of nanomaterials. So far the long-term studies done have been focused on simple exposure, such as working with nanoparticles in a lab or factory setting[1,4]. But that only qualitatively indicates what the exposure from other nanomaterial products could induce. That means that the testing methods need to be just as versatile as the nanomaterials that are being analyzed to ensure consistent exposure studies.

Incidentally, the safety concern is commonly thought of as the secondary reason to conduct the afore mentioned long-term studies. Medical applications of nanomaterials, observed and proposed, were what legitimately piqued the interest of researchers across the world[1]. Already there are multiple FDA approved cancer treatments where nanomaterials are either the targeting mechanism or a part of the active ingredients[1,4,5,6]. Most of these treatments rely on the tendency of cancer cells to be less selective about what passes the cell membrane than regular cells[5,6]. This tendency allows the number of nanomaterial treatment particulates to build-up to toxic amounts in cancer cells while a normal cell might take in a few treatment particles, not enough to cause cell damage[5,6]. However, to date, the nanomaterial treatments are almost exclusively limited to stage three, stage four, and metastatic cancers[6].

The restricted use associated with the nanomaterial treatments comes from the double-edged nature of the cytotoxicity of the treatments[6]. Like most chemotherapy agents, the treatments kill both normal cells and cancer cells and the effective treatments kill the cancer cells faster than the normal cells[6]. Since the true long-term effects of nanomaterials is not known, the approved treatments are restricted to cancer cases where drastic measures are needed to reign in the cancer growth[1,6]. So understanding of long-term effects could allow the expansion of the applicable medical treatment capabilities of nanomaterials.

The nanomaterials that are known to have these medical applications are significantly varied[1,5,6,7,8]. One nanomaterial that was on the forefront of these applications was pure gold nanomaterials. The complexity of the usable shapes and materials has ballooned since the research started, which can be seen by quickly glancing through product catalogues of companies like Sigma-Aldrich.

Another widely anticipated medical nanomaterial set is called a quantum dot[1,7,8]. Quantum dots (QDs) are multiple element nanoparticles which exhibit atom-like properties, most notably being the ability to have electrons move to higher energy states and produce light when returning to the ground state[8]. Many of the elements that are used to make QDs are also used in making semiconductors[8]. Elements such as cadmium, indium, lead, phosphorus, sulfur, selenium, and tellurium are combined as two element pairs or three element compounds in simple QDs[8].

More complex QDs have a simple core dot with another material surrounding the core[8]. The shell compounds have more variety that the elements can be incorporated since zinc sulfide is a common outer shell for QDs[8]. Therefore, the unknown long-term effects of nanomaterials as

well as the inherent complexity of characterizing nanomaterials, such as QDs, require consistent and quick techniques for determining the defining properties of nanomaterials.

Characterization of Nanoparticles

There are four essential characteristics used by researchers when characterizing nanomaterials, and the essential characteristics are listed below.

- Polydispersity Index (PDI) – a measure of the particle size uniformity
- Composition – the elemental makeup of the nanomaterial
- Dimensions – the physical dimensions and geometry of the particles
- Particle Number – the number of particles suspended in a volume of liquid or the number of particles in a weight of powder

Currently, the three "gold standards" for characterizing nanomaterials are electron microscopy, elemental analysis, and surface plasmon resonance[9]. However, each of these characterization tests is only well established for one, possibly two, of the four essential characteristics: electron microscopy determines multiple essential characteristics while the other two methods only determine a single essential characteristic[9].

Surface Plasmon Resonance (SPR) and Dynamic Light Scattering (DLS) are the optimum methods for the polydispersity index (PDI) of the nanomaterial in question[10,11]. DLS is a light scattering method where the Rayleigh scattering of the sample can be used to find an estimate of the particulate size in a sample based on the angle of deflection[10]. The variation in detected sizes can be displayed as a histogram to provide a graphical view of the size dispersion[10]. Then an equation can be used to convert the graphical representation into a single value which is called the polydispersity index. While this makes DLS an easy and inexpensive test to conduct there are certain aspects of nanomaterials that cause uncertainty in the size measurements of the

particulates[10]. This uncertainty comes from the atom-like behavior of most nanoparticles imparted by the relatively similar sizes of true atoms and nanoparticles[10,11].

A common characteristic of nanoparticles is a fluorescence-like property that is called plasmon resonance[11,12]. Plasmon resonance combines the conduction band interactions of the multiple atoms in the nanoparticle with the electron resonance properties of the individual atoms inside the nanoparticle[11,12]. When light of specific wavelengths hit a nanoparticle, electrons are excited into the conduction band and these excited electrons emit photons when they return to their initial ground states[11,12]. While the electrons are excited the small number of atoms in the nanoparticle allows for the electron to move between the atoms via that conduction band[10,12]. This electron motion is observed as a plasma-like layer that glosses over the surface of the nanoparticle[12]. As the light starts to hit the plasma-like electron layer on the nanoparticle both absorption and scattering of the light changes[12]. These changes are what cause the uncertainty in the size estimate from DLS[10,12].

SPR is another simple light-based method that utilizes much of the same calculations that are used with DLS but also takes account of the plasmon resonance[12]. In SPR measurements, an excitation light excites as well as scatters off of the nanoparticles in the sample[11,12]. The reflected light is treated like the scattered light in DLS and the detectors also collect data on the emitted light[11,12]. The main difference between the DLS and SPR is that in SPR the wavelength of the emitted light has a linear correlation to the diameter of the nanoparticles[11,12]. The correlation still has some refinement needed to be precise across measurements on the specific diameter, but the correlation is strong enough that the variation in the diameter is exceptionally well described by the emission spectrum of SPR tests[11,12]. Based on the uncertainty in DLS measurements and the strong correlation between emission wavelength and particle size, SPR is the method that is

considered the best method for measuring polydispersity index with DLS being an acceptable method in lieu of SPR[10,11,12].

Elemental analysis is the second optimum method used with nanomaterials and is used to determine the composition of the nanomaterial. While there are multiple tests that fall under the elemental analysis label, mass spectroscopy (MS) is the set of methods that relate closest to the nanomaterial golden standard[9]. Within the MS method set, literature commonly cites Inductively Coupled Plasma (ICP) and Electrospray Ionization (ESI) varieties of MS in the determination of the nanomaterials composition[13]. This is expected since ICP-MS is consistently used to determine the elemental identities of inorganic samples and ESI-MS is similarly the expected method used to find the elemental identities of organic or complex samples[13]. Based on most of the current literature, ICP-MS is the benchmark standard for the determination of the elemental composition of nanomaterial samples[9,13].

The last two essential characteristics of nanomaterials are particle dimensions or size and number of particles in the sample[9]. Both of these characteristics have the same gold standard test yet two separate methods of conducting the test are required for the different characteristics[9]. The test that is used for these last two characteristics is electron microscopy[9]. When size is the target of a test, Transmission Electron Microscopy (TEM) is considered the optimum method with Scanning Electron Microscopy (SEM) being a suitable quick replacement[9,14]. So the difference between the determination of the two characteristics using either TEM or SEM comes down to the focus of the test[14]. When determining the size of nanoparticles the individual conducting the test is focused on finding a single particle or a set of individual particles that represents the majority of the observed particles in the sample[9,14]. Once the target particle or particles have been found, the operator simply looks to find the clearest close up image of the

target, enabling a precise determination of the three dimensional lengths of the particles[14]. That same operator must reset the sample slide when looking to provide answers about the number of particles in the sample[14]. For this characteristic, the operator is looking to find a representative portion of the slide, called a slide grid, which provides the operator with a simple but effective way to provide a number to the researchers[14]. The number of particles inside the grid is then extrapolated to a particle number for the entire sample based on the number of grids that the slide was broken into during the test[14]. Therefore, even with TEM being the benchmark standard for both particle size and particle number, a researcher still has to effectively run two tests on the same instrument to get the data required for characterization of the nanomaterial[9].

Single Particle ICP-MS (SP-ICP-MS)

Single Particle ICP-MS might be the solution to characterizing nanomaterials with decreased financial investment and increased consistency. SP-ICP-MS is a specialized version of ICP-MS that allows for the analysis of individual particles that are suspended in a liquid sample[15,2]. This happens through quantitatively determining the elemental concentration in each individual particle that is analyzed[15,2]. Single Particle mode analysis is made possible through the use of Time Resolved Analysis (TRA) which is a data collection method that acquires data points rapidly[2,15]. The current capabilities of TRA method provided in the instrument's default software allows for the collection of a data point every 100 microseconds[2,15]. Part of the TRA analysis provided with SP-ICP-MS is the capability to aggregate multiple data points into a peak that can represent a single particle much like how a chromatography peak would be collected and displayed[2,15]. Yet this data aggregation is limited to TRA that is set to record data points less than 300 microseconds apart based on the theory that nanoparticles of any diameter will be

completely detected within a 300 microsecond dwell time, where the dwell time is the time period for each measurement step[2,15]. For TRA that uses dwell times of 300 microseconds or larger, the data points are not aggregated meaning that the intensity of a single data point indicates the entire nanoparticle or the background[15]. These two types of TRA are called Fast TRA and Slow TRA based on whether or not the dwell time input into the software method allows for data aggregation[15].

SP-ICP-MS that uses TRA allows the test that is the gold standard for nanoparticle composition to also become a viable test for determination of particulate size[2,15]. Particulate size can be determined based on the direct correlation of counts from the detector to number of atoms that impacted the detector[15]. The size is determined by using the number of atoms detected and a few preprogramed particle properties to calculate the volume of said particle[15]. Those preprogramed properties are material density, elemental sensitivity, and material to particle ratio[15]. Elemental sensitivity is most commonly determined during a calibration test by having the instrument take measurements of a known ionic solution sample which establishes how many counts from the detector correspond to a known approximate number of atoms of the specified element[15]. Both material density and material to particle ratio are properties that are entered into the software by the operator, which does require some details about the sample to be known prior to starting this analysis[15]. The material to particle ratio is simply a value from 1 to 0 that indicates the percentage of the particle that is made of the material being detected by the instrument[15]. To calculate the spherical volume corresponding to the particle's peak, the intensity is converted to mass of material using the elemental sensitivity[15]. Then the mass of material is converted to volume using the material density before the ratio is used to determine the volume of the entire particle[15]. The software also makes a determination of which peaks are particles and

which are background signals[2,15]. Background Estimated Diameter (BED) is the spherical volume calculation that is associated with the background intensities[2,15]. After the size is calculated the software also records the frequency with which the various sizes of particles are seen throughout the test run[15].

The software provided allows the recorded sizes to be displayed as a histogram[15]. This histogram is practically the same as the plots made from the data that the SPR and DLS methods use to calculate PDI[16], so SP-ICP-MS is again a possible test for replacing a benchmark standard[15]. Even though the histogram is not converted into a PDI value, the histogram is all that a researcher familiar with nanomaterials would need to have a qualitative estimate of that value[15,16]. As the histogram peak becomes narrower, the PDI value gets closer to 0[16]. Whereas when the peak spreads out and resembles the baseline or redistributes into multiple peaks the PDI value gets closer to 1[16].

Along with the histogram, the software calculates the number of particles detected[2,15]. Using the recorded size and frequency data, the software displays the number of particles that were detected hitting the detector during the test[15]. Also the software calculates the particle concentration of the sample using some preprogrammed properties of the instrument and method[15]. The sample test time and flow rate of the sampler are the properties and the software determines the volume of sample tested with these properties[15]. When the volume and the previously found tested number of particles are combined in another calculation the software finds and displays the particle concentration for the sample[15]. Once again this determination of the sample particle concentration indicates that SP-ICP-MS can be used to characterize nanomaterials[2,15].

There is evidence that SP-ICP-MS, or the shared instrumentation if not the methodology, could be a new optimum test in the nanomaterials field. As stated above SP-ICP-MS allows for the determination of a nanomaterial's poly-dispersion index, particulate size, and number of particles[2,15]. The same instrument allows for the determination of the elemental composition via conventional ICP-MS[2,15]. Since all four of the essential properties of nanomaterial characterization can be found with a single instrument after two tests, there is good reason to reconsider the use of three separate instruments and four different tests[15]. Even with the strong case for making SP-ICP-MS the single gold standard test for nanomaterial characterization, the method is a newly developed method[2,15]. This indicates that more research needs to be performed using this technique to ensure that the method can legitimately earn the benchmark standard status[2,15].

Applications of SP-ICP-MS as Described in Literature

In the existing literature that describes the SP-ICP-MS method there are two main groups of papers. One group focuses on the general use of the method, which means that the studies examine several nanoparticle compositions or compare the method to other established characterization techniques[19,21,22,23]. The second group of papers focuses on improving the method for specific purposes, which means that a single nanoparticle composition, and sometimes a single size of nanoparticle, is analyzed during the studies[17,18,20,24]. Both groups of literature are important in legitimizing the need and usefulness of the SP-ICP-MS method. Yet the two approaches cause confusing and possibly contradictory conclusions when new researchers are searching through the literature base.

An example of this contradictory effect is the possibility of lower detection limits[17,18,19,20,21,22,23,24]. While both camps agree that there is an absolute limit to the detection capabilities of SP-ICP-MS there are two different thought processes when the two camps are compared[18,19]. The general use camp indicates that the mathematics demonstrate that we are already achieving the best possible detection limits without creating more sensitive instrumentation[19,21,22,23]. This differs from the specific use camp in that most of the literature produced by this group shows improved capabilities through the addition of extra steps in the analysis process[17,18,20,24]. Adding the process steps does affect the sensitivity of the overall method via reducing the background noise of the samples in the vast majority of papers[17,18,24]. However the addition of steps required specific-use applications is in conflict with the widespread accessibility and reduced costs that the general-use camp strives to maintain[17,18,19,20,22,24].

Another component of the contradictory conclusions gathered from the literature base is related to the conversion of the raw data to analyzed results. Whether the paper comes from the general-use camp or the specific-use camp just about all of the papers that include successful analysis of nanoparticles using SP-ICP-MS incorporate analysis techniques that are not a part of the instrument software or require modifying the instrument software techniques[17,18,19,20,21,22,23,24]. Yet the way that SP-ICP-MS is described in most future use scenarios throughout the literature involves seperate software connected to the instrument analyzing the raw data without modification which maximizes the usefulness of the method[19,21,22,23].

In the general-use literature base, the researcher developed algorithms that provide higher signal-to-noise ratios or refine the formulas for determining specific variables in the SP-ICP-MS calculation scheme. Pace et. al. (2011) focused on refining the formulas for transport or

nebulization efficiency, which is a root variable that nearly all calculation schemes concerning SP-ICP-MS require to function correctly[23]. To be precise, the nebulization efficiency value is what allows the instrument software to determine the particle concentration of a sample after the particle events have been identified[23]. The nebulization efficiency was then refined by continued work from the research group, which allowed for the determination of how nebulization efficiency relates to particle size[21]. These two relationships allow analysts to make characterization determinations on unknown samples, since the size of particle and how numerous the particles are in the sample can be found with one analysis test[21]. Laborda et. al. presented a review of the capabilities of SP-ICP-MS which also went into detail about the mathematics of the method[22]. The mathematical explanations show that sample particle concentration needs to be low enough that a single particle is detected during one dwell period to optimize the Time-Resolved Analysis, size detection is limited by the detection efficiency of the instrument, dissolved concentration and particle mass concentration can be differentiated by analyzing the data pulses in a frequency histogram, and all of the analysis can be done quantitatively or qualitatively based on which formulas the acquired data is run through during data processing[22]. Further research in Lee, et. al. provided a method for estimating the size detection limit for various elements along with some empirical data that correlates to the estimates[19]. The paper shows how to convert the peak intensities into both particle mass and particle diameter using the nebulization efficiency constant, the sensitivity of the instrument and the constant nanoparticle density[19]. From this knowledge base, any individual with an ICP-MS instrument that has Time-Resolved Analysis capabilities can conduct SP-ICP-MS analysis on their samples.

The specific-use group literature tends to start with a specific material to test and then determines the best additions to make for optimizing the analysis of that material. In Touriniemi, et. al., a feasibility study was conducted on environmental samples containing silver nanoparticle[17]. Particles in the 40 nm to 80 nm were optimally detected in a 5 millisecond dwell time with a researcher designed algorithm for analyzing the data that identified peaks of 5 times the standard deviation as nanoparticle events[17]. The work presented by Hadioui, et. al. showed that reducing the dissolved metal concentrations in the sample improves both better resolved nanoparticle peaks and a lower detection limit in their analysis of silver nanoparticles[18]. An ion-exchange column was incorporated into the SP-ICP-MS system as the method for reducing the dissolved metal content in the samples[18]. Hadioui, et. al. again used the ion-exchange column coupled SP-ICP-MS to show that the commercially significant zinc oxide nanoparticle can be analyzed in environmental monitoring settings[20]. During the analysis of wastewater samples, the results showed that there are already some nanoparticles being released into the environment based on tests of unspiked water samples[20]. Upconversion nanoparticles, which are similar to QDs, were the focus of analysis in Meyer, et. al. and an adjustment to the mass filter bandwidth was used to optimize the analysis[24]. This increase of the Quadrupole Mass filter bandwidth allowed for the small diameter particles (10nm) or low mass fraction nanoparticles (less than 5% of nanoparticle by mass) to be detected more consistently when compared to the background noise via an increase of the signal to noise ratio by a multiplier of 3.7[24]. All of the specific-use methodologies do have considerable advantages in the proposed settings.

To conclude, the research into SP-ICP-MS is dispersed in various directions and yet seem to be lacking a focal point aside from analyzing nanomaterials. For prospective researchers there are several routes that can be taken to achieve the goal of characterizing or making

determinations about the target nanomaterials. Unfortunately, there is not a lot of data to show which route of the several is most advantageous for the new researcher.

Project Overview

This project was conducted as part of the effort to establish SP-ICP-MS as a characterization method and bolster the nanomaterial research on Missouri State University campus. The initial stages of the project consisted of standard ICP-MS tests meant to determine the relative amounts of the elements in previously synthesized QDs from the Fichter Lab, which was studying fluorescent indium phosphide core-zinc sulfide shell QDs doped with gadolinium for potential medical diagnostic and therapeutic applications. Since the relative amounts were all the information required the analysis was conducted with the already optimized method of normal ICP-MS. In future research, the analysis could be extended to the use of SP-ICP-MS to measure the sizes of the QDs.

Before utilizing SP-ICP-MS on the Fichter group's QDs, the basic capabilities of the method needed to be established using known samples. A series of SP-ICP-MS measurements were carried out on commercially available gold nanoparticles of varying sizes and these studies were supplemented with DLS and SEM measurements. The overall goal was to create working methods that research groups across campus could benefit from while completing their own nanomaterial research. If a method for SP-ICP-MS measurements is successfully established, the method should be a valuable characterization method that benefits the research on the Missouri State University campus.

MATERIALS AND METHODS

Materials

Quantum Dots from Fichter Lab: Gadolinium doped indium phosphide core with zinc sulfide shell Quantum Dots [Gd:InP/ZnS QDs] (powdered or dissolved in nitric acid) shown in Figure 1, indium phosphide core QDs, were provided by Molly Duszynski of Dr. Fichter's lab

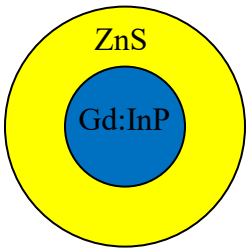

Figure 1. Simple Diagram of a Quantum Dot Particulate with labels.

Gold Nanoparticles: Cytodiagnostics gold nanoparticle – 50 nanometers (stabilized with citric acid in 0.1 mM phosphate buffered saline solution); Sigma gold nanoparticle – 5 nanometers and 10 nanometers (stabilized with citric/possibly tannic acid in 0.02% sodium azide solution); all three of which came from Dr. Bersara of the Physics Department. The age and storage history of these nanoparticle samples was not known. Towards the end of the studies, a 20 nanometers suspension (stabilized in 0.1 mM phosphate buffered saline solution) was acquired from Sigma.

Deionized Water: 18.2 milliohms double deionized (DDI) was provided by a Thermo-Scientific Barnstead E-Pure system.

Nitric Acid: concentrated nitric acid from Sigma-Aldrich

ICP Standards: ICP-grade standards were acquired from various sources: gold (10,000 μg/mL) from SPEX CertiPrep; zinc (10,000 μg/mL), indium (10,000 μg/mL) and phosphorus (10,000 μg/mL) from Ricca; sulfur (10,000 μg/mL) from EM Science; scandium (10,000 μg/mL) from Trace Cert; lanthanum (10,000 μg/mL) from Ricca; cadmium (10,000 μg/mL) from Ricca

Gadolinium Chloride: Gadolinium chloride powder was provided from Dr. Fichter's lab

Other Labware: Micropipettes from Fisher (Fisherbrand); 15 mL and 50 mL polypropylene Falcon tubes were purchased from Fisher, sterile autosampler tubes from Thermo Scientific, reagent bottle dispensing pump.

Sample measurements were conducted on a Mettler Toledo Analytical Balance.

Inductively Coupled Plasma – Mass Spectrometer (ICP-MS) system: Agilent 7900 operating under Mass Hunter software, which could be operated in both standard and single particle modes. Plasma was generated from an Argon gas stream with a forward power of about 1500 kW and a reverse power of about 700 kW with normal operating fluctuations.

Dynamic Light Scattering: NanoBrook Omni Particle Sizer from Brookhaven Instruments

Scanning Electron Microscope: FEI Quanta 200 Scanning Electron Microscope

Methods

QD ICP-MS Solution Preparation. The stock gadolinium solution was made by dissolving 10 mg $GdCl_3$ powder (provided by the Fichter Lab) in 1 mL DDI water, resulting in a 5.97 mg/ml Gd solution. A standard stock solution (SS) was made by pipetting and mixing 2.5 mL from both the indium and the phosphorus standards, 500 μL from both the zinc and the sulfur standards, 210 μL from the gadolinium solution, 37.5 mL of concentrated nitric acid, and bringing to volume with DDI water to make the final 50 mL SS solution which was stored in a

Falcon tube. This mixture was a 500 μg/mL In and P, 100 μg/mL Zn and S, and a 25 μg/mL Gd solution. Then an internal standard solution (ISS) was made by mixing 5 mL of cadmium standard, 5 mL of lanthanum standard, 5 mL of scandium standard, 5 mL of nitric acid, and bringing to volume with DDI water to make a 25 mL ISS solution (2000 μg/mL of Cd, La, and Sc each) which was stored in a falcon tube.

The six calibration standards were 100%, 20%, 4%, 2%, 1%, and 0% solutions using the SS solution as the stock with all six standards having 0.5% of the final volume being from the ISS solution. To make the standards, a volume of SS solution was pipetted out of the stock. Then the volume, along with DDI water, was used in a series of dilutions that made a 20% dilution, a 4% dilution, a 2% dilution, and a 1% dilution. After that the corresponding amount of ISS solution was added to turn the remaining volume, the 20% dilution, the 4% dilution, the 2% dilution, and the 1% dilution into the 100% standard, the 20% standard, the 4% standard, the 2% standard, and the 1% standard respectively. The 0% standard was made by adding ISS solution to a volume of DDI water such that the final concentration of ISS was 0.5%. The composition of the standards is shown in Table 1.

The sample solutions were made from the eleven Quantum Dot samples provided by the Fichter lab and a zinc sulfide powder. Sample labels given here, e.g. 0/75X Gd:InP/ZnS (2/11/19), are as given by the Fichter lab, and represent the different synthetic variations and preparation dates of the samples. Series 1 was analyzed as is from the given sample of 400 μg/mL solution of Gd:InP/ZnS dissolved in a 75% nitric acid solution. Series 2-4 were prepared from about 10 mg of each of the given samples which were then separately dissolved in 50 mL of 75% nitric acid solution to make the series samples. Series 2 was made from the sample 1.0X Gd:InP/ZnS powder and Series 3 was made from the sample 0.75X Gd:InP/ZnS (2/11/19)

powder. Finally Series 4 was made from the sample 0.75X Gd:InP/ZnS (1/20/19) powder. In addition, 4.7 mg of zinc sulfide powder was mixed with about 1 mL of nitric acid and 50 µL of ISS solution then brought the volume of 10 mL with DDI water to make the ZnS sample. Series 5-11 were prepared from 1 - 2 mg of each given sample which were then separately dissolved in 1 mL of nitric acid and 50 µL of ISS solution then brought to the final volume of 10 mL to make the series samples. The given samples that correspond to the series samples are as follows; Series 5 is InP cores in oleylamine, Series 6 is InP/ZnS (nonthesis), Series 7 is 1.0X Gd:InP/ZnS,

Table 1. Composition of Standard Solutions used in the QD ICP-MS Analysis.

Solution Name	**Standard Components (µg/mL)**						**Internal Components (µg/mL)**		
	HNO_3 (%v/v)	Gd	In	P	S	Zn	Cd	La	Sc
Gd Stock	0	5970	0	0	0	0	0	0	0
Standard Stock (SS)	75	25	500	500	100	100	0	0	0
Internal Standard (ISS)	20	0	0	0	0	0	2000	2000	2000
Calibration 100%	20	25	500	500	100	100	10	10	10
Calibration 20%	20	5	100	100	20	20	10	10	10
Calibration 4%	20	1	20	20	4	4	10	10	10
Calibration 2%	20	0.5	10	10	2	2	10	10	10
Calibration 1%	20	0.25	5	5	1	1	10	10	10
Calibration 0%	20	0	0	0	0	0	10	10	10

Series 8 is 1.5X Gd:InP/ZnS, Series 9 is 2.0X Gd:InP/ZnS, Series 10 is Gd:InP/ZnS shell doped, and Series 11 is InP/ZnS (thesis). The sample identities are shown in Table 2. Finally, these samples were remade as needed so that they could be used in ICP-MS analysis.

QD ICP-MS Analysis. The standards and samples that had been prepared were run through an Agilent 7900 series ICP-MS system with autosampler. The test was run using the provided software on a multiple element analysis method.

SP-ICP-MS Sample Preparation. The provided gold nanoparticle (AuNP) solutions were diluted to make working stock solutions that were then used to make all the standards and samples. All three provided AuNP solutions were individually diluted 5000-fold with DDI water (10 μL of solution into a 50 mL volumetric flask that was then brought to volume). After the solution in the flask was well mixed the solution was put into a small amber bottle and labeled as the working stock solution for that particular AuNP. An ionic gold (Au) working stock solution was made by diluting the gold ICP standard to 20 μg/mL. Next the first series of samples were made by diluting 10 μL of the working stock solutions (three AuNP and one Au) to 10 mL with DDI water inside separate plastic test tubes and a reference Au solution was made by transferring the undiluted Au working stock solution to a plastic test tube. The parameters used to test these first series samples were 1.1 L/min of argon, 1550 W of plasma power, 60 seconds for acquisition time, and a 0.0001 second dwell time. All of the parameters except the dwell time are the default settings and the dwell time was chosen to maximize the data points collected with the thought that the extra data points would help in characterizing the smallest of the AuNPs.

The second series of samples were made such that a minimum of 360 nanoparticles were expected to reach the detector so that there would be an appropriate amount of nanoparticle events for analysis with the Single Particle Software. For the 50 nanometer particles, 2 mL of

Table 2. Sample Identities of the Sample Series used in the QD ICP-MS Analysis.

Sample Series	Quantum Dot Particle Type
ZnS	4.7mg Zinc Sulfide powder dissolved in 1mL of Nitric Acid and mixed with 50µL ISS then/brought to 10mL with DDI water
1	Pre-dissolved (75% Nitric Acid) 400µg/mL Gd:InP/ZnS Solution
2	~10mg 1.0X Gd:InP/ZnS powder dissolved in 50mL of 75% Nitric Acid
3	~10mg 0.75X Gd:InP/ZnS (2/11/19) powder dissolved in 50mL of 75% Nitric Acid
4	~10mg 0.75X Gd:InP/ZnS (1/20/19) powder dissolved in 50mL of 75% Nitric Acid
5	1-2mg InP cores in Oleylamine powder dissolved in 1mL of Nitric Acid and mixed with 50µL of ISS then brought to 10mL with DDI water
6	1-2mg InP/ZnS (nonthesis) powder dissolved in 1mL of Nitric Acid and mixed with 50µL of ISS then brought to 10mL with DDI water
7	1-2mg 1.0X Gd:InP/ZnS powder dissolved in 1mL of Nitric Acid and mixed with 50µL of ISS then brought to 10mL with DDI water
8	1-2mg 1.5X Gd:InP/ZnS powder dissolved in 1mL of Nitric Acid and mixed with 50µL of ISS then brought to 10mL with DDI water
9	1-2mg 2.0X Gd:InP/ZnS powder dissolved in 1mL of Nitric Acid and mixed with 50µL of ISS then brought to 10mL with DDI water
10	1-2mg Gd:InP/ZnS shell doped powder dissolved in 1mL of Nitric Acid and mixed with 50µL of ISS then brought to 10mL with DDI water
11	1-2mg InP/ZnS (thesis) powder dissolved in 1mL of Nitric Acid and mixed with 50µL of ISS then brought to 10mL with DDI water

the 50 nm working stock solution was diluted to 10 mL with DDI water and stored in a plastic test tube. A tuning solution for specific calibration of the instrument was made by diluting 500 µL of the Au working stock solution to 10 mL with DDI water and stored in a plastic test tube. Also the sample solutions for the 5 nanometer particles and the 10 nanometer particles did not change from the first series. The parameters used to test these second series samples were 1.1 L/min of argon, 1550 W of plasma power, 60 seconds for acquisition time, and a 0.0003 second dwell time. All parameters were set to default except the dwell time, which was chosen to maintain collection of single nanoparticle events while reducing the data point count to a number that was manageable for hand analysis.

The third series of samples were made such that the expected number of nanoparticles reaching the detector would be approximately equivalent when comparing the different sizes of nanoparticles. The expected number of nanoparticles was calculated using an atoms per particle factor, based on the atomic diameter of gold and reported gold nanoparticle densities, and the reported concentrations of either gold or particles in the original AuNP stocks. For each size of nanoparticle there were four nanoparticle analysis rates chosen to for the desired samples; High rate (H) was about 3000 NP/min, Medium rate (M) was about 1650 NP/min, Low rate (L) was about 300 NP/min, and Ultralow rate (U) was about 150 NP/min. Samples 50L, 10L, and 5H were prepared in the same way that the second series samples were made. 50H was made by diluting 12.5 µL of the original stock solution to 50 mL with DDI water inside a glass volumetric flask then the solution was stored in a labeled amber bottle. 50M was made by diluting 6.89 mL of working stock solution to 10 mL with DDI water in a plastic test tube which is also where the sample was stored. 50U was made by diluting 1 mL of 50L to 5 mL with DDI water in a plastic

test tube which is also where the sample was stored. 10H was made by diluting 76.5 µL of working stock solution to 10 mL with DDI water inside of a plastic test tube which is also where the sample was stored. 10M was made by diluting 42 µL of working stock solution to 10 mL with DDI water in a plastic test tube which is also where the sample was stored. 10U was made by diluting 1 mL of 10L to 5 mL with DDI water in a plastic test tube which is also where the sample was stored. 5M was made by diluting 5.5 µL of working stock solution to 10 mL with DDI water in a plastic test tube which is also where the sample was stored. 5L was made by diluting 5 µL of working stock solution to 50 mL inside a glass volumetric flask then the solution was stored in a labeled amber bottle. 5U was made by diluting 1 mL of 5L to 5 mL with DDI water in a plastic test tube which is also where the sample was stored. The parameters used to test these third series samples were 1.1 L/min of argon, 1550 W of plasma power, 60 acquisition time, and a 0.0003 second dwell time. The parameters were unchanged from the previous series.

The fourth and last series, which was conducted after the corollary studies that are described later in this paper, used a phosphate buffered saline solution to improve the stability of samples and incorporated an additional standard prepared from a freshly acquired 20 nm AuNP solution. A liter solution of 1 mM phosphate buffered saline (PBS) was made by dissolving 1.1484 g of potassium chloride, 0.0962 g of monobasic sodium phosphate, and 0.0284 g of dibasic sodium phosphate in a liter of DDI water. A concentrated stock (355.5 ng/mL) was made for the 20 nm AuNP solution by mixing 336 µL of the original 20 nm solution with 5 mL of 1 mM PBS and bringing the solution to volume in a 50 mL glass volumetric flask before the Concentrated 20 nm stock was stored in a labeled amber bottle. Then a Working 20 nm stock (71.1 pg/ml) was made by mixing 10 µL of Concentrated 20 nm stock with 5 mL of 1 mM PBS and bringing to volume in a 50 mL glass volumetric flask before storing the solution in a labeled

amber bottle. Originally, the Concentrated 20 nm stock and the Working 20 nm stock were made to easily mix a standard solution that would contain about 1 ppb 20 nm AuNPs. Then after reconsidering the particle number contained in a 1 ppb 20nm AuNP solution, the two stocks were used as samples where the 20L sample was made with straight working 20 stock and 20 H sample was made with straight concentrated 20 stock. Both of the 20 nm samples were made and stored in plastic test tubes. 5L sample was made by mixing 1 mL of 1 mM PBS with 9 mL of 5L solution in a plastic test tube. 5 H sample was made by mixing 1 mL of 1 mM PBS with 9 mL of working 5 stock in a plastic test tube. 10L sample was made by mixing 1 mL of 1 mM PBS with 8 µL of working 10 stock and brought to 10 mL with DDI water in a plastic test tube. 10H sample was made by mixing 1 mL of 1 mM PBS with 9 mL of working 10 stock in a plastic test tube. 50L sample was made by mixing 1 mL of 1 mM PBS with 1 mL of 50H solution and brought to 10 mL with DDI water in a plastic test tube. 50H sample was made by mixing 1 mL of 1 mM PBS with 9 mL of 50H solution in a plastic test tube. Also a blank sample was made by mixing 1 mL of 1 mM PBS with 9 mL of DDI water in a plastic test tube. All fourth series samples were vortexed at level 10 for about 10 seconds before being tested. The compositions of all the fourth series solutions are shown in Table 3. The parameters used to test these fourth series samples were 1.1 L/min, 1550 W of plasma power, 60 seconds acquisition time, and a 0.0003 second dwell time. The parameters were again unchanged from the previous series. Finally, all the samples described in this section were remade as needed for the SP-ICP-MS analysis.

AuNP SP-ICP-MS Analysis. The standards and samples were run through an Agilent 7900 series ICP-MS system with autosampler. Each test was run after calibrating the instrument with a provided general tuning solution and a specific Au tuning solution when applicable. The

Table 3. Composition of Solutions used in the fourth series of SP-ICP-MS tests.

Sample Name	Component Quantities	Final Volume
1mM PBS Buffer	1.1484g KCl, 0.0962g NaHPO4, 0.0284g Na2PO4, DDI water	1 Liter
20 Concentrated Stock/20H	336µL 20nm Original Stock, 5mL 1mM PBS Buffer, DDI water	50 Milliliters
20 Working Stock/20L	10µL 20 Concentrated Stock, 5mL 1mM PBS Buffer, DDI water	50 Milliliters
5H	9mL 5 Working Stock, 1mL 1mM PBS Buffer	10 Milliliters
5L	9mL 5L from 3rd Series, 1mL 1mM PBS Buffer	10 Milliliters
10H	9mL 10 Working Stock, 1mL 1mM PBS Buffer	10 Milliliters
10L	8µL 10 Working Stock, 1mL 1mM PBS Buffer, DDI water	10 Milliliters
50H	9mL 50H from 3rd Series, 1mL 1mM PBS Buffer	10 Milliliters
50L	1mL 50H from 3rd Series, 1mL 1mM PBS Buffer, DDI water	10 Milliliters
Blank	1mL 1mM PBS Buffer, DDI water	10 Milliliters

methods were made based on the software Single Particle single element analysis default settings with slight changes. These default settings that ended up being used were the acquisition time (1 minute), various gas flow rates (1.1 L/min of argon), and response factor values (either 200000 CPS/ppb or calculated during method). The default dwell time was increased from 0.1 milliseconds to 0.3 milliseconds to decrease the file size of each test after the first series was

tested and the default density for gold was changed from 19.0 g/mL to 19.37 g/mL to reflect previous literature. The setting changes were made to attempt optimization of the method.

Scanning Electron Microscopy (SEM) Sample Preparation. The first slide prepared for SEM analysis was setup by transferring a few drops of the original stock solution of the 50 nm AuNPs onto an aluminum slide that had copper tape placed on the slide. The solution was dried by touching a corner of a Kimwipe to the drop of solution to remove the excess liquid. Then a methanol solution was added to the location the solution was placed and after a minute the methanol was dried with another Kimwipe. A second slide was prepared using an aluminum slide with copper tape attached and the same sample solution transferred to the tape, with the solution being dried through placement in a Dri-Rite desiccator vessel for about three days. A third slide was prepared using an aluminum slide with carbon tape attached and the original 50 nm AuNP stock solution was transferred onto the tape. The third slide was placed in a Dri-Rite Desiccator vessel for months.

SEM Analysis. The SEM instrument was operated by Dr. Ridwan Sakidja while I observed. After the prepared slide was placed in the instrument and the program indicated everything was operational, the settings were manipulated in order to acquire the clearest SEM image at various positions on the slide.

Dynamic Light Scattering (DLS) Sample Preparation. There were no standards prepared for the DLS method because the software did not require a standard to function properly. The first series of samples were the working stock solutions for the three sizes of AuNPs pipetted into three separate polystyrene absorption cuvettes (2 frosted sides). The second series of samples were 200 μL of the working stock solution for the three sizes of AuNPs diluted to 2 mL with DDI water then transferred into separate polystyrene cuvettes. In the second series

of samples each AuNP size had three samples, so one sample was simply transferred into the cuvette and called unfiltered. Another sample was transferred to the cuvette by being passed through a 0.45 micron nylon syringe filter twice. The third sample was transferred to the cuvette by being passed through a 0.7 micrometer glass fiber syringe filter twice. The cuvettes that held the samples for testing were capped with plastic cuvette caps so that the samples could be stored and reused for every test.

DLS Analysis. The samples were run using a BrookHaven NanoBrook Omni Particle Sizer instrument. A custom method was used for the analysis with the parameters being square polystyrene cell, 60 seconds duration, 25 °C temperature, 10 second equilibration, NNLS (non-negative least squares) data analysis, no dust filter, 0.2 real refractive index, unspecified sample concentration, automatic baseline, and varied configuration and detector angles. After a test the displayed data from the three runs were recorded by hand before setting up the method for the next test. The recorded data was double checked with the electronic records in the software after a series of tests.

Computer Analysis. Attempts to recreate results from SP-ICP-MS tests using the raw data and equations given by the manufacturer of the instrument, were conducted in order to determine how much of the inconsistencies seen in results were from the samples. Equations found in the Single Particle manual were used in conjunction with Excel 2019 to do the calculations. The raw data used in the calculations were the tabulated data sets provided by the tests as well as the input values that correspond to constants used in the calculations.

RESULTS

Quantum Dot Elemental Analysis for Fichter Group Samples

The raw data from the instrument was analyzed in Excel to find the elemental concentrations present in the samples and later the analyzed data from three separate data sets were combined to form the presented data. In this data set the five elements that were supposed to be in the Quantum Dots synthesized by the Fichter lab were selected for detection by the instrument. Those five elements were phosphorus, sulfur, zinc, indium, and gadolinium.

Table 4. Molar Ratios of the five elements detected in the ICP-MS analysis of the Quantum Dot samples.

Sample	[Zn]/[S]	[In]/[P]	[Gd]/[In]	([In]+[Gd])/[P]
ZnS powder	1.28	---------	0.0520	---------
Gd:InP/ZnS	18.3	0.330	0.469	0.485
1.0X Gd:InP/ZnS	0.786	0.302	0.238	0.374
0.75X Gd:InP/ZnS (2/11/19)	0.762	0.270	0.464	0.395
0.75X Gd:InP/ZnS (1/20/19)	0.745	0.269	0.470	0.395
InP cores in Oleylamine	0.580	2.01	0.000137	2.01
InP/ZnS (nonthesis)	0.795	0.493	0.000082	0.493
1.0X Gd:InP/ZnS	0.803	1.53	0.0202	1.56
1.5X Gd:InP/ZnS	0.711	1.04	0.0773	1.12
2.0X Gd:InP/ZnS	0.704	0.569	0.251	0.713
Gd:InP/ZnS shell doped	0.826	0.861	0.0606	0.913
InP/ZnS (thesis)	0.836	0.892	0.0215	0.911

which range from 0.58 to 18.31 with the most frequently seen ratio being around 0.75, show that the balance of sulfur and zinc in the particles is not in line with the expectation for a zinc sulfide shell of a nanoparticle. The logical expectation for inorganic shells on nanoparticles is that the inorganic compound forms a crystalline layer of the compound that interacts with the core in such a way that the core and shell form an ionic bond like interface. That interface is where the cations and anions essentially just change elemental identities in the crystal pattern. Therefore, the ratio of zinc to sulfur should be about 1 for all of the samples in Table 4.

The ratio of indium to phosphorus ranged from 0.27 to 2.01 with the common ratios being about 0.3 and about 0.9. These ratios indicate that the indium to phosphorus balance is also not conforming to the expectations based on the bulk formula. All of the samples in Table 4 should have an indium to phosphorus ratio that ranges from about 0.5 to 1, based on how much gadolinium the indium phosphide lattice incorporated during the specific synthesis method.

The ratios of gadolinium to indium ranged from 0.02 to 0.47, excluding outliers, with the common ratios being about 0.05, about 0.25, and about 0.47. These ratios cannot truly be analyzed like the other three ratios, since the gadolinium content varies in all of the samples based on the synthesis method. The samples also vary with where in the QD the gadolinium was expected to be incorporated, which would mean that gadolinium is not necessarily replacing indium in the crystal lattice.

The ratio of (indium plus gadolinium) to phosphorus range from 0.37 to 2.01 with the most common ratios being about 0.4 and about 0.9. These ratios indicate that there is an imbalance of phosphorus when compared to the combined content of indium and gadolinium in the analyzed particles. The premise of the synthesis was to have gadolinium atoms simply replace a variable amount of indium atoms while maintaining an indium phosphide crystal

structure within the QD. Therefore, the combined indium and gadolinium to phosphorus ratio should have been about 1 in all of the samples shown in Table 4.

There are many possible explanations for these observed elemental imbalances, that range from inconsistent dissolution method to selective dissolution of samples and even include a hypothesis about unexpected synthesis events. One potential reason that the Gd:InP/ZnS (Series 1) sample appears as an outlier is the fact that this sample was provided by the Fichter group as a dissolved solution, while all the other samples were provided as powders that were then dissolved during sample preparation. Because the two sets of digestions were conducted by different individuals possibly using different digestion protocols, the digestion outcomes could be different. These differing outcomes could be from various parameters such as the concentration of acid used, the amount of time the samples were sonicated, how the samples were mixed with the acid, and the ratio of acid to sample in the digestion.

Another explanation for the presented results comes from selective digestion which could be linked to the method of digestion. Since nitric acid was used to digest all the samples and the observations indicate that the cation metals were the elements that are underrepresented. There is a possibility that while in the dissolution matrix the cationic metals form oxides, which are insoluble and caused the liquid autosampler of the ICP-MS instrument to be unable to sample the oxides. This inability to sample all of the given sample would cause the observed skewed elemental contents, however there is no precedent for this variety of dissolution reaction found in literature.

Yet another possible explanation is that an unexpected process in the synthesis could account for the missing cationic metal content of the QDs. There is the logically expected trend that specific materials with equivalent lattice structures will form layered QDs where the lattice

of the core material is continued by the shell material when the QD is synthesized. Based on the intended synthesis method these QDs were supposed to have two layers, which would have been an indium phosphide core and a zinc sulfide shell. The unexpected synthesis comes from the inclusion of the known material phosphorus sulfide in the final QD. Adding phosphorus sulfide into the possible QD materials would convert the two-material structure into a three-material composite. This three-material composite would be made of an indium phosphide core, a phosphorus sulfide interface layer, and a zinc sulfide outer shell. Therefore, the two-material structure assumes that the interface is a clean and fast transition with the first layer of zinc atoms as well as the last layer of indium atoms possibly interacting with both phosphorus and sulfur. The three-material composite assumes that the transition from the InP core to the ZnS shell was not abrupt and the two compositions were separated by a transition layer of sulfur and phosphorus. This separation causes less of the total QD volume to contain the expected cationic metals, which would show elemental results fairly similar to the observed results. If this hypothesis were to be used in the analysis of the observed results, then the conclusion could be made that a thin but significant interface layer was formed during the QD synthesis. However, descriptions of methods for preparing phosphorus sulfide all involve reactions between the elemental forms of phosphorus and sulfur[25,26]. Therefore, there are no examples in literature of ionic phosphorus and ionic sulfur reacting to form phosphorus sulfide as would be required for the hypothesis to be confirmed.

All QD samples that were analyzed for this article were synthesized by the Fichter research group, and there is insufficient information to assess whether there were systemic issues with their preparation that could have led to the large deviations in the composition of the particles compared to the expected compositions or impurities or some other explanation.

SEM of AuNPs

SEM measurements were completed in an attempt to confirm the dimensions of the original AuNP samples. During the session when the first slide was analyzed, an excessive amount of negative charge buildup that decreases the image quality, slide charging, was seen over the vast majority of the slide. There were small isolated regions where structures and particles could be seen. In these regions microparticles were seen, as shown in Image A of Figure 2. While analyzing the second slide the same slide charging effect was observed except that the magnitude of the charging in certain portions of the slide were diminished compared to the first slide. The portions of diminished charging allowed for the visualization of copper phosphate nanoflower structures, shown in Image B of Figure 2, which are believed to be the cause of the surface charging effect. Areas of aggregated 50 nm AuNPs were also found during the analysis of the second slide and are shown in Image C of Figure 2.

Unfortunately, the third slide was never analyzed so there was no clear determination of the extent that the 50 nm particles were aggregated. Even so, the evidence shown here does

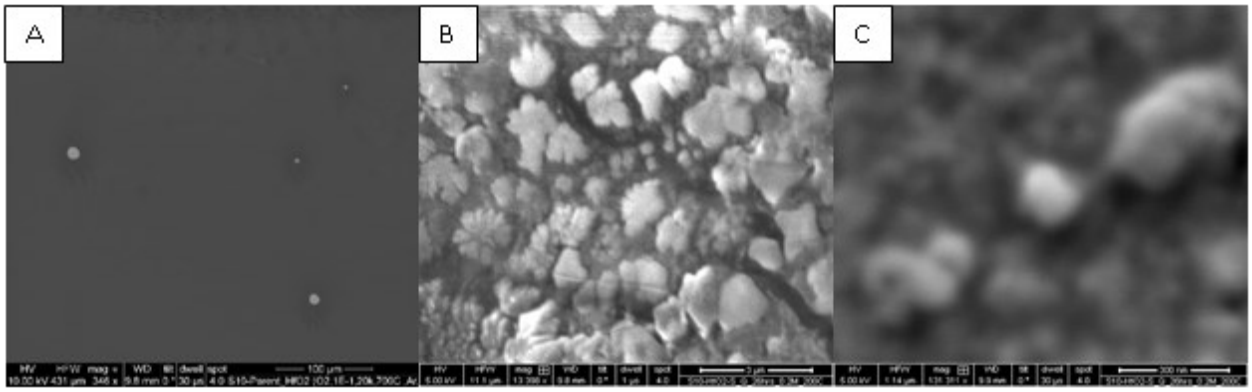

Figure 2. A collection of SEM depicting the results of analysis. Image A shows the observed microparticles seen on the first SEM slide. Image B shows the Copper Nanoflower formations. Image C shows the aggregated nanoparticles seen on the second SEM slide.

indicate that there were aggregated particulates present in the original 50 nm AuNP stock solutions. This means that the samples used in the SP-ICP-MS analysis for 50 nm, 10 nm, and 5 nm are subject to suspicion concerning the accurate size of the particles and number of particles in the samples.

SP-ICP-MS

While the results displayed by the SP-ICP-MS software was not captured in an image. An example of the results display, with a few missing columns, is shown in Table 5. In Figure 3, there is an example of a particle size histogram is depicted.

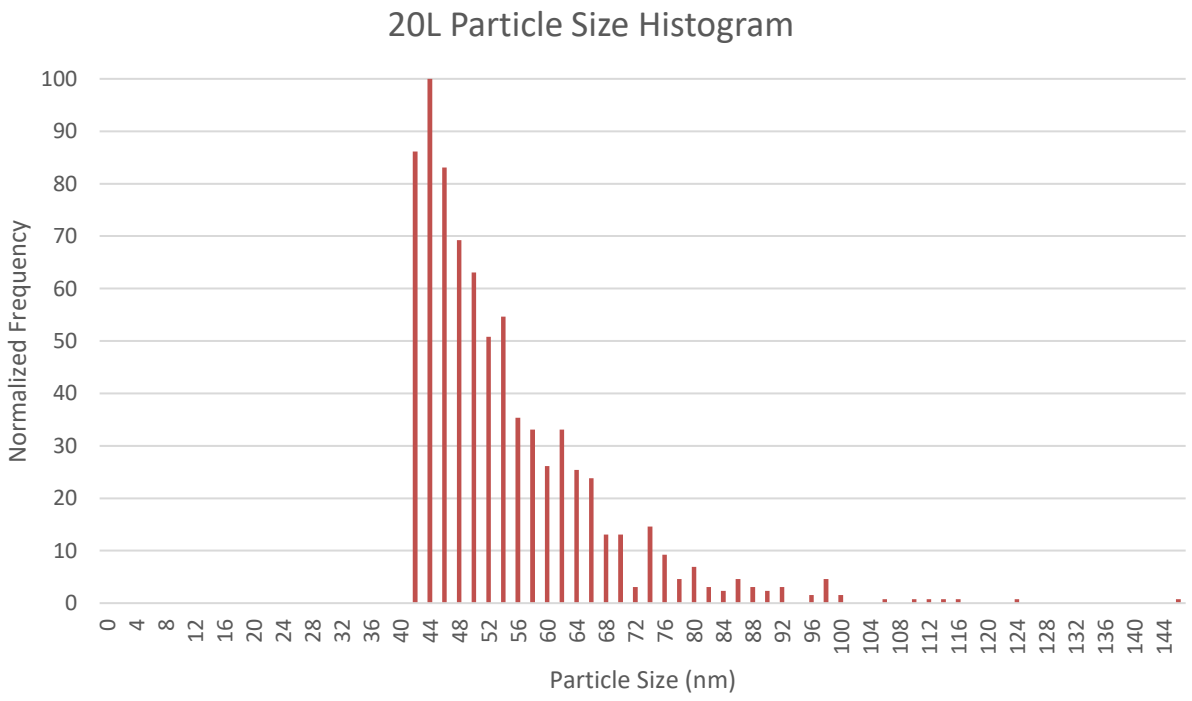

Figure 3. Example Histogram of 20L Sample Shown in the Results Display Above.

Table 5. Example of Results Display for a SP-ICP-MS Run

Type	Sample Name	Nebul. Eff.	# of Particles	Particle Conc. (particles/l)	Mass Conc. (ng/l)	Ionic Conc. (ppb)	BED (nm)	Median Size (nm)
IonicBlk	PBS					0		
IonicStd (AN)	Au ref					20		
IonicBlk	PBS							
RM	20 ref	0.004	1115	7.90E+08	64	<0.0000	2.34	17
Sample	PBS	0.004	238	1.70E+08	18.6	<0.0000	8.58	18
Sample	5 L sample	0.004	437	3.10E+08	43.3	<0.0000	9.65	20
Sample	10 L sample	0.004	332	2.30E+08	17.1	<0.0000	7.74	17
Sample	20 L sample	0.004	1014	7.20E+08	1313.1	0.0516	10.59	49
Sample	50 L sample	0.004	230	1.60E+08	25.8	<0.0000	9.43	19
Sample	PBS	0.004	53	3.70E+07	3.4	<0.0000	6.92	16
Sample	5 H sample	0.004	872	6.20E+08	382.3	18.5066	24.13	38
Sample	10 H sample	0.004	487	3.40E+08	242.8	20.586	24.93	38
Sample	20 H sample	0.004	3515	2.50E+09	47353.2	345.9865	62.34	117
Sample	50H sample	0.004	1949	1.40E+09	685.2	0.3355	11.15	28

The first series was an attempt to use default parameters and concentrations to determine what kind of work was needed to optimize SP-ICP-MS on the instrument available. The observed results showed BEDs (Background Estimated Diameters) and average sizes that

Table 6. Average Particle Size and Average Background Estimated Diameter for the first series of SP-ICP-MS samples.

Sample Name	Average Size (nm)	Average BED (nm)
50 RM	33 ± 12.75	8.81 ± 0.53
50 nm	44 ± 36.12	7.94 ± 1.66
10 nm	24.67 ± 3.30	7.77 ± 0.84
5 nm	21 ± 3.74	7.75 ± 1.94

differed from expected values. The observed particle sizes for the first series samples were either in tight groups around 21 nm and 25 nm or disperse groupings around 44 nm and 33 nm, as shown in Table 6. Both the 44 nm and the 33 nm groupings were for the same 50 nm sample, which was a solution that was supposed to contain about 8.9 pg/ml of gold in the form of 50 nm AuNPs according to the manufacturer. The difference between the RM and nm samples was simply the calculation method that the software used when analyzing the raw data points. The approximately 25 nm grouping was from the 10 nm sample, which was a solution that was supposed to contain about 11.6 pg/ml of gold in the form of 10 nm AuNPs according to the manufacturer. Also, the 21 nm grouping was from the 5 nm sample, which was a solution that was supposed to contain about 11.6 pg/ml of gold in the form of 5 nm AuNPs according to the manufacturer. In all four of the analyzed data sets there was an observed BED of about 8 nm, which was a problem considering that 8 nm is larger than the smallest expected sample and over three-fourths the size of the middle expected sample. This set of results seemed to indicate that the SP-ICP-MS technique would be applicable to larger nanoparticles and caused the researchers to speculate that there was aggregation in the samples, as these results were acquired before the SEM measurements were taken.

Table 7. Average Particle Size and Average Background Estimated Diameter for the second series of SP-ICP-MS samples.

Sample Name	Average Size (nm)	Average BED (nm)
50 RM	47 ± 0.71	7.16 ± 0.47
50 nm	21.67 ± 0.94	2.9 ± 0.54
10 nm	8.67 ± 1.89	2.13 ± 0.37
5 nm	10.67 ± 2.05	2.87 ± 0.57

The second series had concentrations such that a low but measureable number of particles were detected during a sample test. These results were more reliable but still differed from the expected values. The observed particle sizes for the second series samples were in four tight groups at the size values of 47 nm, 22 nm, 9 nm, and 11 nm, as shown in Table 7. In this series both the 47 nm group and the 22 nm group were again from the same 50 nm sample solution, which was a solution that was supposed to contain 1.78 ng/ml of gold in the form of 50 nm AuNPs. This concentration of material was supposed to ensure that at least 360 particles would be analyzed during the 1-minute timeframe that the samples were tested, which means that there is at least 6 nanoparticle events analyzed per second throughout the test. The 9 nm grouping was from the 10 nm sample solution, which was supposed to contain 11.6 pg/ml of gold in the form of 10 nm AuNPs. This concentration of material was supposed to ensure that at least 360 particles would be analyzed during the 1-minute timeframe that the samples were tested. The 11 nm grouping was from the 5 nm sample solution, which was supposed to contain 11.6 pg/ml of gold in the form of 5 nm AuNPs. This concentration of material is to ensure that at least 360 particles would be analyzed during the 1-minute timeframe that the samples were tested. The

observed BED sizes were more acceptable with this series at about 3 nm or about 2 nm for all three AuNP samples and about 7 nm for the RM sample. This set of results indicated that with optimization SP-ICP-MS could be a technique used for all sizes of nanoparticles, since the basic optimization efforts of increasing the sample to noise ratio in the data and tuning the instrument to be more sensitive to gold caused results with more acceptable standard deviations as well as BEDs that were not overwhelming compared to the expected sizes of the tested particles. But the variation seen with the particle sizes for the 50 nm solution samples and the average particle size found for the 5 nm sample made it clear that the AuNP original solutions needed to be investigated for aggregation, after this series of samples were run the SEM tests were started.

The third series had concentrations where equivalent numbers of particles were detected during a run for all three of the sample types. The data showed good BEDs like the second series and average sizes that were closer to the expected values. The RM sample was changed to the 10 nm AuNP samples, since the intended use of SP-ICP-MS was to continue investigating materials like the QDs that were used earlier, which have a diameter of 3.5 nm. Also a calibration check conducted at the midpoint of the calibration curve is commonly more effective than a check that uses an endpoint solution. The observed particle sizes for the third series samples were seven fairly well grouped sets at the size values of 36 nm, 30 nm, 11 nm, 10 nm, 9 nm, and two groups at about 8 nm, as shown in Table 8. The 36 nm and the 30 nm groups were from two samples that had different concentrations of gold but were all in the form of 50 nm AuNPs from the same stock solution. The 11 nm and the 10 nm groups were from two samples that had different concentrations of gold but were all in the form of 10 nm AuNPs from the same stock solution. The 9 nm group and one of the two 8 nm groups were from two samples that had different concentrations of gold but were all in the form of 5 nm AuNPs from the same stock solution. The

Table 8. Average Particle Size and Average Background Estimated Diameter for the third series of SP-ICP-MS samples.

Sample Name	Average Size (nm)	Average BED (nm)
10 RM	7.75 ± 0.43	2.98 ± 0.56
50 L	35.8 ± 12.2	5.71 ± 0.362
50 U	30 ± 11.19	4.1 ± 1.69
10 L	10.8 ± 3.76	3.58 ± 1.08
10 U	10 ± 4.20	4.08 ± 1.80
5 L	8.8 ± 3.19	4.21 ± 1.91
5 U	8 ± 3.95	3.38 ± 1.36

last set of particles sizes grouped at about 8 nm was from the same sample that formed the 11 nm group but the software used a different set of equations to convert the raw data into results since this was the data points of the RM sample. The observed BED sizes seen were higher than the second series values at about 4 nm with an outlier of about 6 nm but were still acceptable for determining the size of the tested AuNPs. This set of results indicates that SP-ICP-MS is capable of determining expected values with a good calibration sample is used to set up the run. Overall, there was a trend that the more concentrated a solution used for sampling was the higher the values for the observed particle sizes were determined to be.

The fourth series had the 20 nm AuNP sample added to provide a more reliable reference material to base the software calculations on as well as the addition of PBS to attempt to increase the stability the analyzed samples. An effective increase in stability for the analyzed samples would simply have been a cessation of continued aggregation or a reversal of observed aggregation. This series still showed results that differed from expected values. The observed

particle sizes for the fourth series samples were seven disperse groupings, one tight grouping, and three single data points. The seven disperse groupings were at particle size values of 90.5 nm, 58 nm, 50 nm, 45.5 nm, 41.5 nm, 32.5 nm, and 27 nm, as shown in Table 9. The three single data points were particle sizes of 28 nm, and two of 38 nm, and the one tightly grouped set was at 17 nm, as shown in Table 9. The 90.5 nm and 58 nm groups as well as the 28 nm data point were all from samples that had varying concentrations of the same solution that contained the 50 nm AuNPs. The 41.5 nm and 17 nm groups were from the same sample solution that contained the 20 nm AuNPs. The 50 nm and 32.5 nm groups as well as one of the 38 nm data point were all

Table 9. Average Particle Size and Average Background Estimated Diameter for the fourth series of SP-ICP-MS samples.

Sample Name	Average Size (nm)	Average BED (nm)
20 RM	17 ± 1.63	3.76 ± 1.44
50 H	28	11.15
50 L	58 ± 39	16.22 ± 6.79
50 U	90.5 ± 12.5	21.91 ± 1.87
20 L	41.5 ± 7.5	12.74 ± 2.15
10 H	38	24.93
10 L	32.5 ± 15.5	17.07 ± 9.33
10 U	50 ± 7	16.47 ± 2.95
5 H	38	24.13
5 L	27 ± 7	12.48 ± 2.83
5 U	45.5 ± 11.5	17.25 ± 3.27

from samples that had varying concentrations of the same solution that contained the 10 nm AuNPs. The 45.5 nm and the 27 nm groups as well as the other 38 nm data point were all from samples that had varying concentrations of the same solution that contained the 5 nm AuNPs. The observed BED size ranged from 25 nm to 11 nm in this series with an outlier of about 4 nm for the RM sample. Using the newest AuNP as the calibration material in this series seems to have shown that there was aggregation present in all three of the original nanoparticle solutions. One interesting development from the results of this fourth series is that the trend of increasing particle size with increasing concentration has transitioned into a parabolic trend where the minimum of the curve is when about 300 particles per minute are being analyzed. Which implies that there is an optimum particle number around the 300 particles per minute value where the number of nanoparticle events are isolated enough that the program can easily distinguish the nanoparticle event data points from noise data points, but frequent enough that noise data points are not misidentified as nanoparticle event data points. The evidence from the BED indicates that the PBS solvent increases the ambient noise of the measurement even when a blank containing PBS is used, which is unfortunate since there seemed to be a stability problem with the test samples in this study.

These stability problems, or evidence of aggregation, have a few known sources and solutions. First, the longer that a NP solution is stored after the synthesis occurs the more individual NPs will bond to other individual NPs creating more and more aggregates. The interaction that causes the Au in two separate individual NPs to start the bonding of the two NPs is an extension of the hydrophobic effect where the ionic coating on the individual NPs weakens such that the Au on the surfaces of the NPs is pressured into coalescing. Secondly, the same hydrophobic effect causes aggregation when a NP solution is diluted because the ionic coating

diffuses off of the individual NP surfaces to maintain the ionic equilibrium of the solution. Therefore, the fact that the three original solutions were old and had unspecified storage conditions for that duration make the conclusion that the solutions were aggregated reasonable if not highly probable.

DLS

DLS measurements were conducted to correlate how monodispersed the original AuNP samples were during SP-ICP-MS testing and to verify that there were signs of degradation in the samples. There were two sets of numbers that came out as data and those two numbers were effective diameters and PDI values. For the 50 nm unfiltered samples the effective diameter varied from 58.94 nm to 1920.71 nm with two frequently seen diameters, which were 115 nm and 60 nm. The 10 nm unfiltered samples had effective diameters that ranged from 32.70 nm to 1869.76 nm with the three most frequently seen diameters being 1300 nm, 1000 nm, and 33 nm. The 5 nm unfiltered samples had effective diameters ranging from 38.30 nm to 3898.23 nm with the three most frequently seen diameters being 1050 nm, 700 nm, and 40 nm. Table 10 shows the raw data from the unfiltered sample tests.

The 50 nm nylon filtered samples had effective diameters ranging from 0.00 nm to 2282.04 nm with the three most frequently seen diameters being 1250 nm, 750 nm, and less than 1 nm. The 10 nm nylon filtered samples had effective diameters ranging from 0.15 nm to 562.67 nm with three most frequently seen diameters being 450 nm, 40 nm, and less than 1 nm. The 5 nm nylon filtered samples had effective diameters ranging from 0.27 nm to 2512.14 nm with the three most frequently seen diameters being 400nm, 39 nm, and less than 1 nm. Table 11 shows the raw data from the nylon-filtered sample tests.

Table 10. Raw data from the DLS analysis of Unfiltered Samples.

Sample	Effective Diameter (nm)			Poly-dispersion Index Values		
Name	**Run 1**	**Run 2**	**Run 3**	**Run 1**	**Run 2**	**Run 3**
50 nm	91.21	1087.08	93.24	0.286	0.259	0.295
50 nm	1435.49	2598.75	127.65	0.334	0.0533	0.28
50 nm	1920.71	113.25	115.07	0.225	0.276	0.208
50 nm	117.54	111.70	119.57	0.196	0.209	0.194
50 nm	63.04	59.85	59.79	0.148	0.176	0.183
50 nm	58.94	59.93	59.08	0.161	0.145	0.168
10 nm	8054.54	2577.57	3673.80	0.986	0.502	0.623
10 nm	635.08	469.06	495.11	0.446	0.372	0.470
10 nm	915.96	1036.35	941.31	0.006	0.224	0.0.92
10 nm	1296.68	1869.75	1321.98	0.941	3.935	1.025
10 nm	32.70	34.94	33.32	0.368	0.373	0.383
10 nm	33.50	33.35	33.13	0.384	0.400	0.375
5 nm	10645.02	5889.86	1820.60	0.569	0.300	0.382
5 nm	1085.8	800.98	960.09	0.249	0.187	0.215
5 nm	407.68	398.20	378.08	0.469	0.485	0.446
5 nm	1047.38	3898.23	1068.19	0.512	33.452	1.437
5 nm	740.15	724.73	689.35	0.312	0.353	0.367
5 nm	38.50	38.47	38.31	0.315	0.309	0.304
5 nm	41.63	41.05	41.39	0.308	0.329	0.297

The 50 nm glass fiber filtered sample had effective diameters ranging from 56.21 nm to 60.39 nm with the most frequently seen diameter being 59 nm. The 10 nm glass fiber filtered sample had effective diameters ranging from 234.67 nm to 346.73 nm with the most frequently

Table 11. Raw data from the DLS analysis of the Nylon-Filtered Samples.

Sample	Effective Diameters			Poly-Dispersion Values		
Name	**Run 1**	**Run 2**	**Run 3**	**Run 1**	**Run 2**	**Run 3**
50 nm	1.28	0.08	0.19	0.389	0.233	0.436
50 nm	713.34	1215.39	814.23	0.394	0.551	0.461
50 nm	1052.15	756.34	1330.28	0.493	0.395	0.604
50 nm	0.15	0.00	0.41	0.341	0.000	0.361
50 nm	2282.04	25.71	1606.28	0.833	0.651	0.680
10 nm	417.48	556.28	564.27	0.400	0.486	0.526
10 nm	0.29	0.26	0.45	0.362	0.293	0.455
10 nm	0.26	436.75	0.15	0.407	0.417	0.302
10 nm	37.50	36.95	41.82	0.419	0.411	0.408
10 nm	42.70	40.96	42.22	0.401	0.424	0.405
5 nm	1.02	623.24	1769.42	0.376	0.540	0.289
5 nm	2512.14	0.27	341.77	0.131	0.085	0.354
5 nm	306.76	474.11	496.8	0.324	0.459	0.485
5 nm	38.93	40.30	39.37	0.337	0.310	0.301
5 nm	38.99	39.44	39.19	0.321	0.313	0.328

seen diameter being 300 nm. The 5 nm glass fiber filtered sample had effective diameters ranging from 42.21 nm to 48.87 nm with the most frequently seen diameter being 45 nm. Table 11 shows the raw data from the glass fiber filtered sample tests. In Table 12, a summary of the effective diameter data along with averages and sample breakdown is shown.

The 50 nm unfiltered samples PDI ranged from 0.145 to 0.276 with the average PDI being 0.191. The 10 nm unfiltered samples PDI ranged from 0.006 to 3.935 with the average PDI being 0.709 and the average PDI excluding outliers being 0.456. The 5 nm unfiltered samples PDI ranged from 0.297 to 33.452 with the average PDI being 3.191 and the average PDI excluding the outliers being 0.440. Table 10 shows the raw data from the unfiltered sample tests.

The 50 nm nylon filtered sample PDI ranged from 0.000 to 0.833 with the average PDI being 0.455 nm and the average PDI excluding outliers being 0.461. The 10 nm nylon filtered sample PDI ranged from 0.293 to 0.527 with the average PDI being 0.408. The 5 nm nylon filtered sample PDI ranged from 0.085 to 0.540 with the average PDI being 0.330. Table 11

Table 12. Raw data from the DLS analysis of the Glass Fiber Filtered Samples.

Sample	**Effective Diameters**			**Poly-Dispersion Values**		
Name	**Run 1**	**Run 2**	**Run 3**	**Run 1**	**Run 2**	**Run 3**
50 nm	60.39	60.24	59.56	0.161	0.182	0.176
50 nm	56.21	57.72	59.25	0.181	0.181	0.155
10 nm	308.54	346.73	304.36	0.329	0.362	0.341
10 nm	234.67	283.67	299.34	0.281	0.305	0.343
5 nm	42.21	47.48	48.87	0.202	0.094	0.082
5 nm	45.03	42.18	43.83	0.199	0.285	0.252

shows the raw data from the nylon-filtered sample tests.

The 50 nm glass fiber filtered sample PDI ranged from 0.155 to 0.182 with the average PDI being 0.173. The 10 nm glass fiber filtered sample PDI ranged from 0.291 to 0.362 with the average PDI being 0.329. The 5 nm glass fiber filtered sample PDI ranged from 0.082 to 0.285 with the average PDI being 0.186. Table 12 shows the raw data from the glass fiber filtered sample tests. In Table 13, a summary of the PDI value data along with averages and sample breakdown is shown.

As there is a high variance shown in all six sets of data presented from the DLS analysis, in conjunction with the relatively high precision seen in each individual set, little effort is needed to infer that the three original samples used for the SP-ICP-MS analysis were not ideal materials for the work that was intended. In all three sample preparation methods, the results showed that the effective diameters and PDI values of the three AuNP solutions varied significantly while up to two different samples were tested throughout the entire analysis of the DLS methodology. This consistent trend of variation seen when comparing the different sample preparation methods indicates that the original solutions were to blame for the results as opposed to the DLS method. With the variations seen in the effective diameters being on the scale of order of magnitude versus standard deviation there is high probability that the three original solutions were affected by size altering effects. These specific size altering effects that might be affecting the solutions could be a few known phenomena such as Oswald Ripening or aggregation, both of which would explain the increased overall particle size and the significantly varied particle size results. Oswald Ripening explains the data because in this phenomenon the material that makes up the particles in solution transfers between particles to cause individual particles to grow or shrink toward the size extreme that the particle is closer to when the ripening begins. Aggregation

Table 13. Ranges and Averages of the Effective Diameters and PDI values for each of the DLS Samples.

Sample	Filter	Effective Diameter (nm)			Poly-dispersion Index Values		
Name	Name	Range	Average	Std Dev	Range	Average	Std Dev
50 nm	Unfiltered	58.94-2598.75	460.66	744.87	0.0533-0.334	0.211	0.066
50 nm	Nylon	0-2282.04	653.19	706.46	0-0.680	0.455	0.192
50 nm	Glass Fiber	56.21-60.39	58.90	1.48	0.155-0.182	0.173	0.011
10 nm	Unfiltered	32.70-8054.54	1304.90	1899.80	0.006-3.935	0.661	0.838
10 nm	Nylon	0.15-564.27	147.89	212.07	0.293-0.526	0.408	0.057
10 nm	Glass Fiber	234.67-346.73	296.22	33.48	0.291-0.362	0.329	0.024
5 nm	Unfiltered	38.31-10645.02	1466.41	2472.40	0.187-33.452	1.981	7.042
5 nm	Nylon	0.27-2512.14	450.78	705.87	0.085-0.540	0.330	0.113
5 nm	Glass Fiber	42.21-48.87	44.98	2.47	0.082-0.285	0.186	0.075

explains the data because there should be some particles of the original size still present in solution even after the aggregate size has grown substantially compared to the original particle size. When looking at the variations seen in the PDI value results there is significant evidence that the original solutions are no longer monodispersed solutions, which is indicated by the single diameter value given by the manufacturer on the label but have aged into poly-disperse solutions. Overall, there is considerable evidence showing that the sample solutions were not the expected monodisperse nanoparticle solutions, which means that the sample solutions are the most likely cause for the troubles seen in acquiring repeatable SP-ICP-MS data. Now whether the trouble came from the variable size, the variable consistency in particles, or some mixture of both would require an in-depth analysis of the original solutions that was not conducted in this set of research.

Computer Analysis

This analysis was conducted in the attempt to better understand how the software running the SP-ICP-MS tests was calculating results for these runs and to see if that provided any insights into the observed inconsistent results. To start the analysis, an understanding of the data flow and calculations were gathered by studying the ICP-MS MassHunter Workstation Single Nanoparticle Application book which was provided with the instrument and software. The formulas that the software uses to calculate the results were used as shown in the book or rearranged to be used in the analysis. An overview of the data flow that occurs in the software is shown in Figure 4.

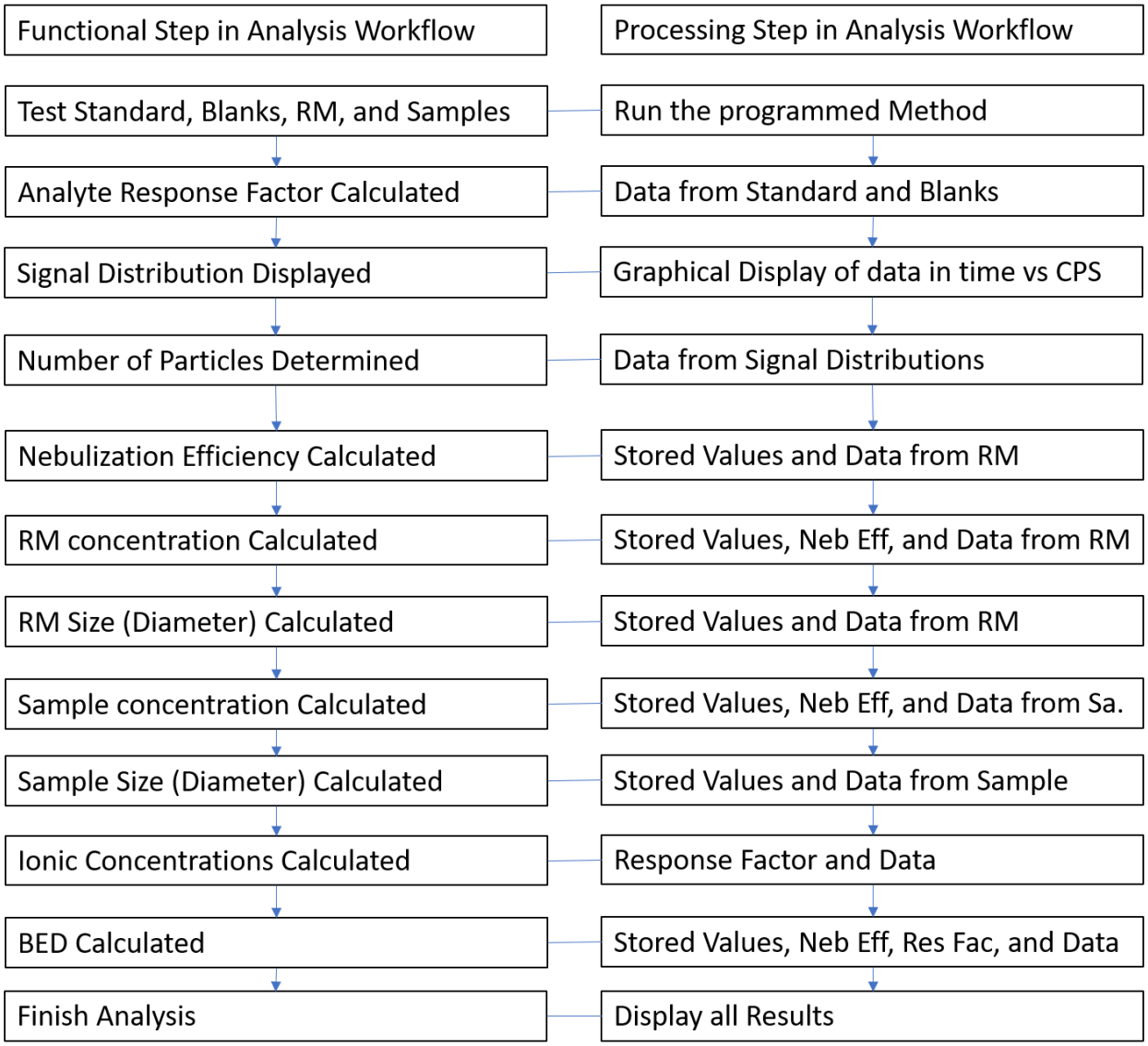

Figure 4. Schematic showing the Analysis Data Workflow of the software used with the SP-ICP-MS instrumentation.

The calculations in the analysis were completed in the order that the software is expected to conduct the calculations. That way the comparison of the hand derived data and the computer-generated data is as directly relatable as possible in their raw forms. Therefore, the first parameter calculated was the Response Factor (s). In the software, s is the value used to convert a signal peak into a comparable amount to the analyte substance based on experimental standards

tested during the course of the method. Initially the *s* was calculated using the average signal intensity of the Au+ (I_{Ion}), the average signal intensity of the blanks (I_{blk}), and the known concentration of the Au+ solution (C_{Ion}) as shown in Equation 1.

Equation 1. Response Factor formula

$$s = \frac{(I_{Ion} - I_{blk})}{C_{Ion}}$$

These initial calculations resulted in a *s* value of around 1450 CPS/ppb, which means that each ppb of Au from the sample that is introduced to the nebulizer is expected to produce a detector response of 1450 Counts collected Per Second. When comparing the initial hand-derived *s* value to the default *s* value, the hand-derived *s* value seemed low but reasonable compared to the default *s* value of 20000 CPS/ppb. This *s* value was compared to the computer-generated value, which was back calculated from the Nebulization Efficiency (η_n).

Back-calculating *s* from η_n required some rearrangement of equations since the applicable equations for η_n did not include *s* as a factor. The equation used to calculate η_n based on the RM concentration, which is the route used by the software during the conducted experiments, is shown in Equation 2. In Equation 2, N_p is number of particles detected and *T* is the time of analysis run and *V* is the sample flow rate and C_{std} is the concentration of the RM solution while m_{std} is the calculated mass of an individual RM particle.

Equation 2. Nebulization Efficiency formula that uses the Reference Material Concentration

$$\eta_n = \frac{N_p}{\left(\frac{C_{std} \times 10^3}{m_{std}}\right) V(T)}$$

Equation 3 shows the equation used to calculate η_n based on the RM size, which is useful in this scenario because of the presence of *s* in the equation. In Equation 3, d_{std} is the diameter of the RM particles and ρ_{std} is the density of the RM inside the particles and *s* is the response factor of the analyte element and I_p is the peak intensity of the RM sample and t_d is the integration time and V is the flow rate and f_d is the molar fraction, which represents how much of the total RM particle the analyte element composes.

Equation 3. Nebulization Efficiency formula that uses the Reference Material Size

$$\eta_n = \frac{\left(\frac{4}{3}\pi\right)\left(\left[\frac{d_{std}}{2}\right]^3\right)\rho_{std}(s)60}{(I_p)t_d(V)f_d(10^{12})}$$

In order to find the computer-generated value for *s*, Equation 2 and Equation 3 were set equal to each other and then the entire argument was solved to equal *s*. After solving the argument for *s* the equation that defines the Standard Particle Mass ($m_{std,}$ fg), shown as Equation 4, was used to simplify the solved equation.

Equation 4. Standard Particle Mass formula

$$m_{std} = \left(\frac{4}{3}\pi\right)\left(\left[\frac{d_{std}}{2 \times 10^7}\right]^3\right)\rho_{std}(10^{15})$$

The result of solving and simplifying the argument is shown in Equation 5.

Equation 5. Response Factor formula back-calculated from Nebulization Efficiency formulas

$$s = \frac{\eta_n(I_p)t_d(V)f_d(10^{12})}{\left(\frac{4}{3}\pi\right)\rho_{std}\left(\left[\frac{d_{std}}{2}\right]^3\right)60}$$

When the known values of 0.0003 sec for t_d, 0.364 ml/min for V, 1 for f_d, 20 nm for d_{std}, 19.37 g/cm^3 for ρ_{std} and the given values of 0.004 for η_n, 6095842 CPS for I_p were input into Equation 5 the computer-generated value of s was found to be 546949 CPS/ppb.

The s value generated by the instrument's software is only about 0.3% of the value from Equation 5, and the source of the discrepancy is not clear, and may simply reflect variations in units used not clarified in the software documentation. This conclusion was reached by considering that both the s value and the η_n value are constants as well as the fact that the determined values are inconsistent.

Therefore, the thought occurred that possibly the software integrated the peaks in the raw data to form the data used for the calculations made by the software. After manually going through one entire sample's worth of data and conducting a rough estimate of the integration process. The hand integrated data was again analyzed for the necessary values, which were then compared to the values found for the same variables in the nonintegrated raw data to determine if integrating the raw data actually aided in making the software calculations match the hand derived calculations. The comparison showed that the values for the variables practically stayed the same, with the major difference being that the integrated values were a little less consistent than the nonintegrated values when comparing the values to the software given values.

Since the attempts to rectify the hand-derived s value with the computer-generated s value were unfruitful, the decision was made that a return to the basics was necessary. The basic

that was chosen for study was the m_{std}, partly because this value is not supposed to change unless the diameter of the RM and/or the density of the RM changes. Both the diameter and the density of the RM are parameters that the researcher is supposed to input into the software while creating the method for running tests on their samples. In the case of the current test being analyzed the RM diameter was input as 20 nm and the density of the RM was input as 19.37 g/cm^3. So the hand derived m_{std} was calculated to be 0.081 fg according to Equation 4, which is how the software is supposed to calculate m_{std}.

To determine if the software was using the same value for the m_{std}, the m_{std} was back-calculated from the η_n. Equation 2 was rearranged to solve for m_{std} as shown in Equation 6.

Equation 6. Standard Particle Mass formula rearranged from Nebulization Efficiency formula (Equation 2)

$$m_{std} = \frac{\eta_n(V)T(C_{std} \times 10^3)}{N_p}$$

After inputting the known values of 20000 ng/L for C_{std}, 0.39 ml/min for V, 1 min for T and the given values of 0.004 for η_n, 1115 particles for N_p into Equation 6 a m_{std} value of 26.117 fg was found. Once again a significant difference in numerical values for a variable was found when comparing the hand derived value to the computer generated value.

With the failed attempt to rectify m_{std} values in conjunction with the inability to rectify s values, the conclusion was reached that the software is analyzing data in a manner that is not consistent with the manual given by the software provider. This inconsistency could be from some underlying calculation that the software is conducting in the background that affects the displayed results. Or this inconsistency could result from the specific interactions between the coding logic and the analysis instrumentation, which could be causing a manipulation of values in an unexpected way compared to the workflow shown in Figure 4. A third possible cause of the

inconsistency is that formulas in the given manual are not the same formulas that the software is using during analysis. No matter what the true cause of inconsistencies are there is ample evidence that there is a need for reworking the analysis software of SP-ICP-MS before the method is ready for practical research use.

CONCLUSIONS

Analysis of QDs from Fichter Lab

The main goal of the collaboration with the Fichter lab was accomplished as there was a successful analysis of composition data. As shown in the results section, the ICP-MS analysis of the provided QDs was completed and the bulk formula of the QDs were found. Even though the ratios of the 5 elements in the QDs were found to be unexpected compared to the predicted bulk formulas, empirical bulk formulas were determined through the analysis. Any further research concerning the QD bulk formulas would need to come about through the Fichter lab, as that research group knows what procedures were used in the synthesis of the QDs and what can be done to troubleshoot the synthesis process. Another aspect of the need for the Fichter lab to be involved in further research is that there is an unknown need for achieving the expected bulk formulas of the QDs. However, continued collaboration is not possible because the Fichter research lab has been disbanded.

Suitability of SP-ICP-MS for Characterizing NPs

The data as well as the previously known features indicate that the original intention of showing that SP-ICP-MS has the potential to become the next generation of gold standard characterization methodology for nanomaterials is achievable, even with this study not providing confirming data. This indication of achievable status comes from the previously known features of SP-ICP-MS claiming that all four of the essential characteristics of nanoparticles can be estimated, if not determined. In addition to the claim, the data showed that all four characteristics are calculated or displayed during analysis even if the data in question did not show good reproducibility all four characteristics did have values or displays given from each analysis.

Unfortunately, the computer analysis that was completed attempting to recreate the displayed results from the raw data and the provided equations was not as successful as desired to confirm the full extent of the original intention, as shown previously in the results section. So, while the current capabilities of the method do not fulfill the full extent of the original expectations, the idea that SP-ICP-MS is the next step in analytical nanomaterial methodology can still be inferred via the completed analysis on multiple nanomaterials.

Problems with how the software converts the raw data to the displayed values comprise this researcher's current reasoning for the method not being in widespread current use. An inability to determine the value of the response factor from the raw data is at the heart of the software problems, especially since the response factor determinations would logically occur in the calibration portion of a testing run and the fact that the value is a foundational aspect of the current calculations. This could mean that the provided equations are not strictly followed by the software or that the software applies the provided equations in a manner that is inconsistent with the logic schemes provided alongside the equations. Either way that scenario would necessitate the standardization of the calculation suite for the technique to be functional in the proposed use.

All together SP-ICP-MS has been shown to provide a more manageable method for nanomaterial characterization when compared to the current best techniques, assuming that well-synthesized nanoparticles are used as standards. With the capability to test at least three of the four, if not all, required characteristics in a single test both time and monetary investments are decreased. In addition to decreasing investments for the characterization of nanomaterials, the single test provides the opportunity for nearly all studies done on these materials to use a single method, which will greatly increase consistency in results and aid in reproducibility studies. In conclusion, SP-ICP-MS is a single technique that is capable of providing characterization data

with decreased investment from researchers, once the calculation methods used in accompanying softwares are optimized to succinctly analyze the raw data into software display values.

REFERENCES

1. Bridges, J., De Jong, W., Jung, T. & Rydzynski, K. Risk Assessment of Products of Nanotechnologies. Risk Assessment of Products of Nanotechnologies. *European Commission* (2009).

2. Khin, M., Nair, A., Babu, V., Murugan, R. & Ramakrishna, S. A review on nanomaterials for environmental remediation. *Energy & Environmental Science* **5**(8). 8075. (2012).

3. Sennac, S. Single particle analysis of nanomaterials using the Agilent 7900 ICP-MS. *Agilent Technologies, Inc*. (2014). at https://grupobiomaster.com/wp-content/uploads/2015/05/1285.pdf

4. Tiny Considerations for Working with Nanomaterials. (2019).

5. Bae, K., Chung, H. & Park, T. Nanomaterials for cancer therapy and imaging. *Molecules and Cells* **31**, 295-302 (2011).

6. Pillai, G. Nanomedicines for Cancer Therapy: An Update of FDA Approved and Those under Various Stages of Development. *SOJ Pharmacy & Pharmaceutical Sciences* (2014). doi:10.15226/2374-6866/1/2/00109

7. Fernandez-Fernandez, A., Manchanda, R. & Mcgoron, A. J. Theranostic Applications of Nanomaterials in Cancer: Drug Delivery, Image-Guided Therapy, and Multifunctional Platforms. *Applied Biochemistry and Biotechnology* **165**, 1628–1651 (2011).

8. Bera, D., Qian, L., Tseng, T.-K. & Holloway, P. H. Quantum Dots and Their Multimodal Applications: A Review. *Materials* **3**, 2260–2345 (2010).

9. Richman, E. & Hutchison, J. The Nanomaterial Characterization Bottleneck. *ACS Nano* **3**, 2441-2446 (2009).

10. Kato, H., Nakamura, A., Takahashi, K. & Kinugasa, S. Accurate Size and Size-Distribution Determination of Polystyrene Latex Nanoparticles in Aqueous Medium Using Dynamic Light Scattering and Asymmetrical Flow Field Flow Fractionation with Multi-Angle Light Scattering. *Nanomaterials.* **2**, 15-30 (2012).

11. Nguyen, H., Park, J., Kang, S. & Kim, M. Surface Plasmon Resonance: A Versatile Technique for Biosensor Applications. *Sensors.* **15**, 10481-10510 (2015).

12. Zeng, S., Baillargeat, D., Ho, H. & Yong, K. Nanomaterials enhanced surface plasmon resonance for biological and chemical sensing applications. *Chemical Society Reviews* **43**, 3426 (2014).

13. Meermann, B. & Nischwitz, V. ICP-MS for the analysis at the nanoscale – a tutorial review. *Journal of Analytical Atomic Spectrometry* **33**, 1432-1468 (2018).

14. Inkson, B. Materials Characterization Using Nondestructive Evaluation (NDE) Methods. *Woodhead Publishing* 17-43 (2016). at https://www.sciencedirect.com/science/article/pii/B978008100040300002X

15. MassHunter Workstation Single Nanoparticle Application. *Agilent Technologies, Inc.* (2017).

16. Okuda-Shimazaki, J., Takaku, S., Kanehira, K., Sonezaki, S. & Taniguchi, A. Effects of Titanium Dioxide Nanoparticle Aggregate Size on Gene Expression. *International Journal of Molecular Sciences* **11**, 2383-2392 (2010).

17. Touriniemi, J., Cornelis, G. & Hassellöv, M. Size Discrimination Capabilities of Single-Particle ICPMS for Environmental Analysis of Silver Nanoparticles. *Anal. Chem.* **84**, 9, 3965-3972 (2012).

18. Hadioui, M., Peyrot, C. & Wilkinson K.J. Improvements to Single Particle ICPM by the Online Coupling of Ion Exchange Resins. *Anal. Chem.* **86**, 10, 4668-4674 (2014).

19. Lee, S., Bi, X., Reed, R.B., Ranville, J.F., Herckes, P. & Westerhoff, Paul. Nanoparticle Size Detection Limits by Single Particle ICP-MS for 40 Elements. *Environ. Sci. Technol.* **48**, 17, 10291-10300 (2014).

20. Hadioui, M., Merdzan, V. & Wilkinson, K.J. Detection and Characterization of ZnO Nanoparticles in Surface and Waste Waters Using Single Particle ICPMS. *Environ. Sci. Technol.* **49**, 10, 6141-6148 (2015).

21. Pace, H.E., Rogers, N.J., Jarolimek, C., Coleman, V.A., Gray, E.P., Higgins, C.P. & Ranville, J.F. Single Particle Inductively Coupled Plamsa-Mass Spectrometry: A Performance Evaluation and Method Comparison in the Determination of Nanoparticle Size. *Environ. Sci. Technol.* **46**, 22, 12272-12280 (2012).

22. Laborda, F., Bolea, E. & Jiménez-Lamana, J. Single Particle Inductively Coupled Plasma Mass Spectrometry: A Powerful Tool for Nanoanalysis. *Anal. Chem.* **86**, 5, 2270-2278 (2014).

23. Pace, H.E., Rogers, N.J., Jarolimek, C., Coleman, V.A., Higgins, C.P. & Ranville, J.F. Determining Transport Efficiency for the Purpose of Counting and Sizing Nanoparticles via Single Particle Inductively Coupled Plasma Mass Spectrometry. *Anal. Chem.* **83**, 24, 9361-9369 (2011).

24. Meyer, S., Gonzalez de Vega, R., Xu, X., Du, Z., Doble, P.A. & Clases, D. Characterization of Upconversion Nanoparticles by Single-Particle ICP-MS Employing a Quadrupole Mass Filter with Increased Bandpass. *Anal. Chem.* **92**, 22, 15007-15016 (2020).

25. Hudson, R.B. (1957). *Method of Continuously Producing a Phosphorus Sulfide* (US2794705A). *U.S. Patent and Trademark Office*. https://patents.google.com/patent/US2794705A/en

26. Griffith, E.J., Ngo, T.M. (1995). Process for Preparing Sulfides of Phosphorus (US5464601A). *U.S. Patent and Trademark Office*. https://patents.google.com/patent/US5464601A/en